Green Synthesis of Nano-Activated Carbon from Reed Stalk – Characterization and Evaluation Performance in Phenolic Water Treatment

Article *in* Ecological Engineering & Environmental Technology · August 2024

DOI: 10.12912/27197050/191952

CITATIONS
0

READS
83

5 authors, including:

Ass. Prof. Rana Abbas Azeez
University of Technology_Iraq
27 PUBLICATIONS **174** CITATIONS
SEE PROFILE

Firas K. Al-Zuhairi
University of Technology - Iraq
34 PUBLICATIONS **182** CITATIONS
SEE PROFILE

Shahnaz Bassim
University of Technology, Iraq
3 PUBLICATIONS **17** CITATIONS
SEE PROFILE

Muayad M. Hasan
University of Technology, Iraq
11 PUBLICATIONS **17** CITATIONS
SEE PROFILE

EEET ECOLOGICAL ENGINEERING & ENVIRONMENTAL TECHNOLOGY

Ecological Engineering & Environmental Technology 2024, 25(10), 306–323
https://doi.org/10.12912/27197050/191952
ISSN 2299–8993, License CC-BY 4.0

Received: 2024.06.10
Accepted: 2024.08.15
Published: 2024.09.01

Green Synthesis of Nano-Activated Carbon from Reed Stalk – Characterization and Evaluation Performance in Phenolic Water Treatment

Rana Abbas Azeez[1], Shahnaz B. Khazal[1], Firas K. Al-Zuhairi[2], Muayad M. Hasan[1*], Zaidoon M. Shakor[2]

[1] Oil and Gas Engineering Department, University of Technology - Iraq, Baghdad, Iraq
[2] Chemical Engineering Department, University of Technology - Iraq, Baghdad, Iraq
* Corresponding author's e-mail: muayad.m.hasan@uotechnology.edu.iq

ABSTRACT

During the past few decades, interest in phenolic substances in aquatic environments has increased due to their wide uses in numerous industries despite their high toxicity. This study aimed to investigate removing phenol from contaminated wastewater using synthesized nanoscale-activated carbon (AC) as a sorbent. The AC was synthesized from reed stalks as a local bio-based material using a chemical activation approach. X-ray diffraction (XRD), scanning electron microscopy (SEM), and energy dispersive X-ray (EDX) in addition to the Fourier transform-infrared spectroscopy (FTIR) were applied to characterize the synthesized AC. The study tested four different factors using the experimental statistical design, data analysis with Design Expert Software, and a central composite design (CCD) using response surface methodology (RSM) to maximize phenol elimination. These factors involved initial phenol concentration (ranging from 30 to 120 ppm), pH levels (ranging from 2 to 11), concentration of adsorbent range from 50 to 600 ppm, and reaction time range from 30 to 120 minutes. These variables were used as input data for the prediction model to determine the removal efficiency (%) of phenol. The analysis of the ANOVA was conducted to examine the model performance. The analysis results suggested that the most effective model in explaining the process of phenol elimination was the second-order quadratic model, and the predicted data strongly matched the experimental values. The findings revealed that the optimal adsorption conditions obtained from the experimental work were initial phenol concentration of 30 $mg \cdot L^{-1}$, adsorbent dose of 600 $mg \cdot L^{-1}$, pH equal to 2, reaction time of 120 minutes, and the capacity of the adsorption was 30.0825 $mg \cdot g^{-1}$. As a consequence, the nano-activated carbon extracted from reed stalks effectively adsorbs phenol from wastewater.

Keywords: phenol, nano-activated carbon, adsorption, plant waste, wastewater, organic pollutants.

INTRODUCTION

Recently, environmental issues have had the most attention of worldwide concern due to a growing amount of harmful compounds in wastewater that negatively affect ecological life [Al-Nini et al., 2023; Saeed, et al., 2020]. Recently, environmental issues have had the most attention of worldwide concern due to a growing amount of harmful compounds in wastewater that negatively affect ecological life [Al-Nini et al., 2023; Saeed, et al., 2020]. The clean water provision represents a financial and environmental challenge. Therefore, it is necessary to implement suitable management techniques to disregard the harmful impact of water pollution and advance a sustainable future [Al-mahbashi et al., 2022; Ajala et al., 2022; Leal et al., 2019]

With recent developments in technology and industries, different forms of pollution have caused great suffering in the environment, population health, and natural resources sustainability because of various toxins released into the environment. Therefore, eliminating sources of

pollution is considered a tactical issue in environmental protection to advance development in sustainable [Ewis and Hameed, 2021].

Organic pollutants discharged from the petrochemical and refinery sectors are major sources of environmental pollution [Ragothaman and Anderson, 2017; Singh and Singh, 2019]. Phenol is a considerable organic contaminant often present in the effluent from these sectors [Qiu et al., 2022]. Moreover, it is one of the main components of industrial wastewater and can also be found in home wastewater, and agricultural runoff, in addition to various industries such as disinfectants, plastic, rubber proofing, pharmaceuticals, steel, coal gasification, and plastic production [Zhang et al., 2021] interest in the toxicological and environmental impacts of this component has grown Therefore, there has been an increase in interest related to the toxicological and environmental effects of this particular component [Roberts et al., 2022; Zhang et al., 2021].

Phenolic chemicals are highly soluble in water and stable, allowing them to accumulate in the food chains of aquatic creatures, potentially causing harm. Phenol is discharged from industrial sectors at contaminant concentrations between 0.1–6.800 mg/L [Mishra et al., 2023; Wang et al., 2021]. Consequently, it should be restricted to the acceptable human use limit of 3.5 mg/L [Patil and Arya].

Various techniques and processes have been developed to eliminate phenols from wastewater released from oil and petrochemical industries. These methods comprise chemical precipitation, filtration, flocculation, ion exchange, electrochemical treatments, physical adsorption, chemical oxidation, and solvent extraction. They are frequently employed to remove metal ions and organic compounds from wastewater [Qasem et al., 2021; Chai et al., 2021]. In the adsorption process, the phenol particles stick to the solid surface to be removed from the effluent [Almahbashi et al., 2021]. During the chemical oxidation process, phenol is separated by chemical agents such as ozone gas to initiate oxidation reactions. In contrast, the extraction method uses a solvent to dissolve phenol and separate it from the aqueous phase. Finally, in the electrochemical process, electrical current and specific electrodes are used to break down and remove the phenol; the efficiency of these methods depends mainly on the electrochemical reactions at the electrodes [Junet al., 2019]. There are a lot of flaws and shortcomings with standard procedures and processes, especially when it comes to implementation strategies and high costs. Thus, it is necessary to develop effective strategies to get around these problems [Alara et al., 2021]. The drawbacks of these techniques are low selectivity, generating waste sludge that needs additional treatment, high operating costs, and many technical issues, particularly at low pollutant concentrations [Saravanan et al., 2021].

The adsorption technique of all the sophisticated remediation methods is the most effective and profitable choice since it has many benefits in phenol removal including high efficacy in eliminating, flexibility in handling of adsorbent materials, and simplicity in execution. Moreover, being environmentally friendly since it avoids the production of harmful byproducts and eliminates the need for complex infrastructure in treatment systems [Al-mahbashi et al., 2023; Kutty et al., 2019]. In addition, it is considered a suitable option for large-scale treatment of wastewater generated from petrochemical industries [De Farias et al., 2022]. Different adsorbent materials such as zeolite, activated carbon, transition metal oxides, agricultural residues, clay, and other natural and manufactured adsorbents were used in this method [Dehmani et al., 2022]. Commercial adsorbents are an efficient material, but it is limited in practical uses due to the high production and fabrication costs. Consequently, there is a growing need to develop less expensive substitute adsorbents which can offer comparable or even higher removal efficiencies to reduce pollutants in the water.

From economic and environmentally friendly viewpoints, the reuse of agriculture waste that is locally available, abundant and cost-effective, as a precursor for the synthesis of eco-friendly adsorbent has been greeting attention. This way provides valuable materials and minimizes solid waste. The activated carbon synthesized from plant waste is characterized as an effective adsorbent for many scientific research since it has a high surface area and porosity [Oruç et al., 2019].

The generation process includes many steps and, the main step is the activation process, which is carried out chemically using agents like oxidants and dehydrates or physically with agents like steam or CO_2. The chemical activation method integrated with KOH was used to synthesize the activated carbon from a nutshell for adsorption of phenolic wastewater [Naji and Tye, 2022; Da Silva et al., 2023]. Melo et al., 2024 examined the impact of chemical activation utilizing $ZnCl_2$ at 20% w/w for 12 hours on the activity

of activated carbon extracted from olive pits by pyrolysis. The produced AC was used as a sorbent for eliminating phenol from wastewater. From the equilibrium analysis, they demonstrated that as the temperature rose, the capability of the phenol to absorb increased to a maximum value of around 120 mg. Moreover, the thermodynamic analysis has shown a spontaneous, favorable, endothermic, and entropy-controlled manner for phenol adsorption on the activated carbon. Mohammadi et al., 2022 presented the efficiency of magnetized activated carbon (MAC) using iron oxide nanoparticles extracted from tea leaves to eliminate phenol from the aqueous solution by the adsorption process. The study was conducted on different variables such as iron content, extract volume, time, and temperature, applying Design Expert 10 software to analysis of the process. The results illustrated that the high activity of MAC toward phenol removal from the water reached 98%.

Allahkarami et al., 2023 tested the effectiveness of phenol removal from wastewater and the adsorption capacity of premium Acacia magnum wood activated carbon (AMW-AC), which was made by activating H_3PO_4 at the temperature of 900 °C, 45 min activation time, and activating agent concentration of 40%. The results presented that the maximum phenol removal and highest adsorption capacity were about 73% and 53.8 mg/g respectively at a temperature of the solution of 25 °C, a contact period of 138 minutes, the initial concentration of the phenol of 150 ppm and 3 pH of the solution.

The study aimed to develop a novel technique for removing phenol from contaminated wastewater using activated carbon nanoparticles (ACNPs) derived from reed stalks. The research used a chemical activation process to optimize the conditions for maximum phenol adsorption and explore the influence of different factors. Through experimental design and statistical analysis, the study showed the potential of ACNPs as an effective and sustainable solution for wastewater treatment.

METHODOLOGY

This research involves the green synthesis of nanomaterials from reed stalks and consists of several steps. These steps start with washing the reed stalks with distilled water, cutting and drying them, and proceeding to the chemical activation. Figure 1 shows a flowchart for the synthesis of green nanocarbons.

Materials

Plant – reed stalks were collected from agriland in Dujail City, Iraq.

Chemicals – hydrochloric acid (HCl) and NaOH were supplied by Sigma-Aldrich, USA.

Nano-carbon synthesis

In the present study, nano-scale activated carbons were synthesized through a chemical activation route [Gayathiri, 2022; Johnson, 1999]. Initially, reed stalks were cleaned with distilled water and thence allowed to soak for 12 hours to remove contaminants. Then, it was dried at 100 ± 5 °C for 24 hr. After that, milled and sieved to 300 µm. The resulting powder was treated with 1 *M* NaOH at 100 °C for 1 hr with continuous stirring at 500 rpm, followed by placing the sample in an oven to dry. Thereafter, the sample was carbonized at

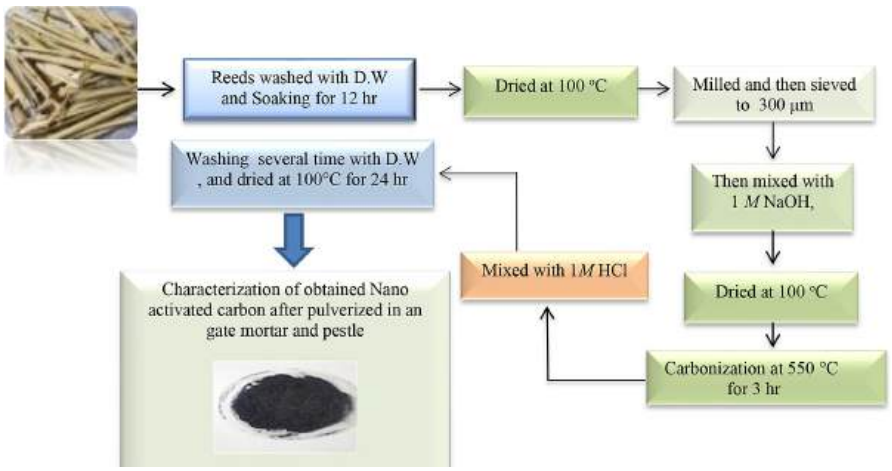

Figure 1. Flowchart of green synthesis of nano-activated carbon

550 °C in a furnace in an oxygen-free furnace. The furnace was then permitted to cool down to ambient temperature. Next, the obtained material is purified with 1 *M* HCl for 1 hour with continuous stirring at 500 rpm, then filtered, washed multiple times with distilled water, and moved to be dried in a lab dryer at 100 °C for 24 hr. Lastly, the obtained material was pulverized in an agate mortar for further characterization.

Batch adsorption studies

The phenol adsorption was performed as a model pollutant using a batch system and synthesized ACNPs as adsorbents in an aqueous solution. Different doses of adsorbent, ranging from 50 to 600 ppm, were screened into 100 mL at an initial phenol range concentrations of 30–120 ppm, in a conical flask of 250 mL, and stirred at 110 rpm in a rotary shaker. The study examined the effect of acidity ranging from pH 2 to 11 on the adsorption technique, as a result of contact time with two different times of 30 and 120 minutes at a temperature of 25 °C. The solution pH was adapted to the required level by adding 0.1 N HCl and 0.1 N NaOH. The phenol solution concentration was calculated employing a UV spectrophotometer with 500 nm wavelength. Equation 1 was applied to estimate the adsorption capacity q(t) (mg/g) of the phenol amount per unit mass of adsorbent at a given time (t) [Azeez and Al-Zuhairi, 2022].

$$q(t) = q(t) = \frac{(Ci - Ct)V}{m} \quad (1)$$

where: Ci – the initial phenol concentration in ppm, Ct – the concentrations of phenol and at any time in ppm., V – the volume of the phenol in the sample, m – the adsorbent (ACNPs) weight.

Characterization of adsorbent

An X-ray diffractometer (XRD) examination was implemented on the produced carbon nanoparticles utilizing a Bruker Meas Srv (D2-208219)/D2-2082019 diffractometer apparatus from Bruker AXS in 8 Billerica, MA, USA.

Energy-dispersive X-ray (EDAX) analysis employing a Quanta TM 450 FEG equipment from Oxford Instruments in the USA and scanning electron microscopy (SEM) using a JoeL 6360LA apparatus were conducted to examine the microstructure of the synthesized ACNPs. Additionally, A spectroscopy of Fourier transform–infrared (FTIR) type (Bruker Tensor 27 instrument, Germany) was applied to characterize the functional groups present in the ACNPs produced before and after the elimination 3 of phenol. The alkalinity and acidity degrees were measured by a pH meter (WTW, Germany).

RESULTS AND DISCUSSIONS

Characterizations of nano-activated carbon

The crystalline nature of the synthesized ACNPs was analyzed using the XRD test as shown in Figure 2. The XRD test is performed to analyze deeply the structural materials. The XRD test of biosynthesized nano-activated carbon displays wide peaks at ~ 25.8° and ~ 43°(weak) diffraction angles, almost comparable to the XRD results of standard activated carbon which has two peaks at diffraction angles of ~24° and ~44° (weak) diffraction angles [Ryanto et al., 2020]. From Figure 2, it was noticed that the dominant structure, in the absence of sharp peaks on the activated carbon diffractogram, was amorphous. In amorphous

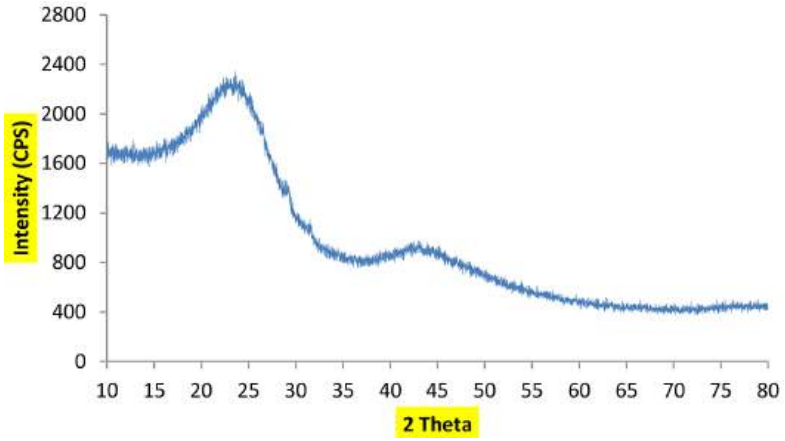

Figure 2. XRD pattern of as-prepared activated carbon NPs

materials, there is more free space and cavities than in crystalline materials leading to high adsorption capacity [Moralı et al., 2018; Fadhil et al., 2017].

Figure 3 (a, b) elucidates the structure of biosynthesized nano-activated carbon using a scanning electron microscope (SEM). Figure 3 shows that activated carbon forms of lignocellulose carbon are more effective and have desirable morphologies with particle sizes between 28 and 60 nm. Meanwhile, Figure 3c illustrates that the distribution of bio-activated carbon size is within the nanoscale range, with 72.1 nm average diameter. The biosynthesis of AC from cellulosic materials claims that materials based on cellulose can make AC with non-uniform and irregular (amorphous) carbon particles; additionally, carbon particles produced Nano-sized [Azeez and Al-Zuhairi, 2022; Lee et al., 2013].

Moreover, the EDS elemental analysis results mapping of the synthesized Nano-activated carbon is illustrated in Figure 4, which contains C, O, Na, mg, Si, and Al elements. It was determined that all elements were homogeneously distributed. As can be seen in Figure 3a, the activated carbon is essentially synthesized from cellulose material as a feedstock. Thus, the intense presence of C and O is a predictable result [González-García, 2018]. The results obtained were closely comparable to those stated by Liang et al. in 2020., which found that AC synthesized from coconut shells had higher C and O wt%.

The FTIR analysis was applied to recognise the functional groups of the nanosized activated carbon as depicted in Figure 5. The broad peak of 3422.6 cm^{-1} is related to O–H group bands attributed to the H_2O molecules vibration [Saleh and Danmaliki, 2016]. The observed peak at 1697 cm^{-1} relates to the C=O bending of R-COOH [Baikousi et al., 2012]. The band 1467 cm^{-1} overlaps to the asymmetrical and symmetrical C-H stretched vibrations. The large peaks from 900 to 1300 cm^{-1} represent the weak band due to the presence of the C–O group in the sample [Liu et al., 2017]. Furthermore, the peak at 875 cm^{-1} is

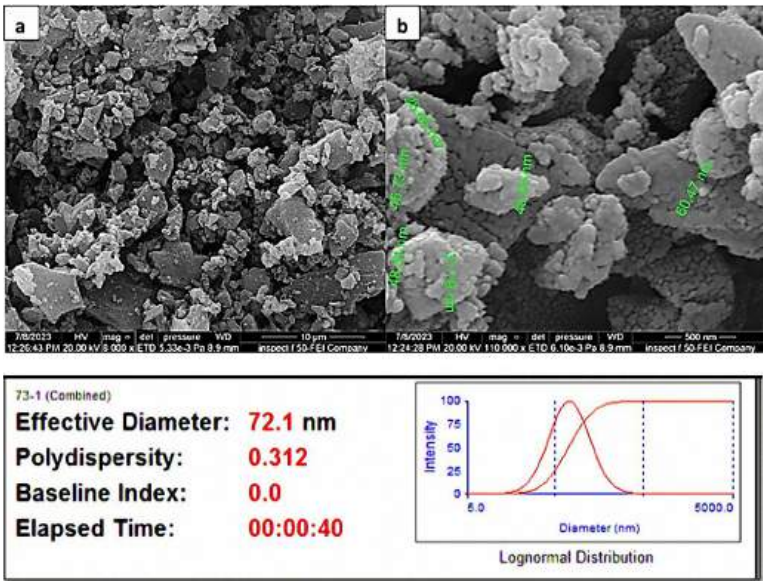

Figure 3. (a, b) SEM, (c) particle size distribution of AC biosynthesized

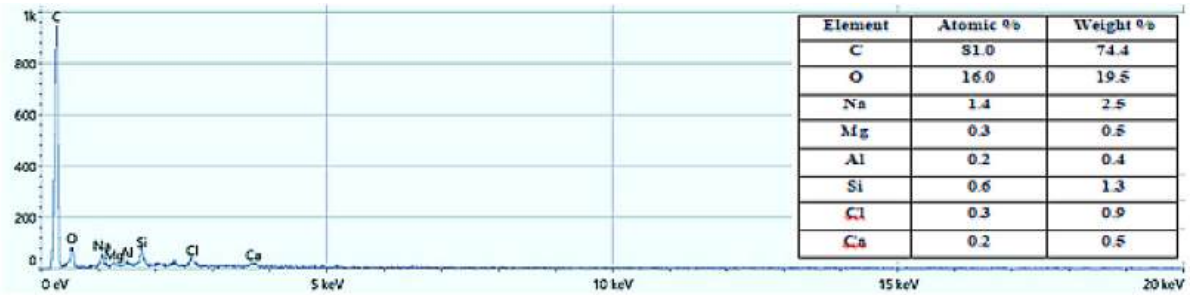

Element	Atomic %	Weight %
C	81.0	74.4
O	16.0	19.5
Na	1.4	2.5
Mg	0.3	0.6
Al	0.2	0.4
Si	0.6	1.3
Cl	0.3	0.9
Ca	0.2	0.5

Figure 4. EDS analysis of nano-activated carbon biosynthesized

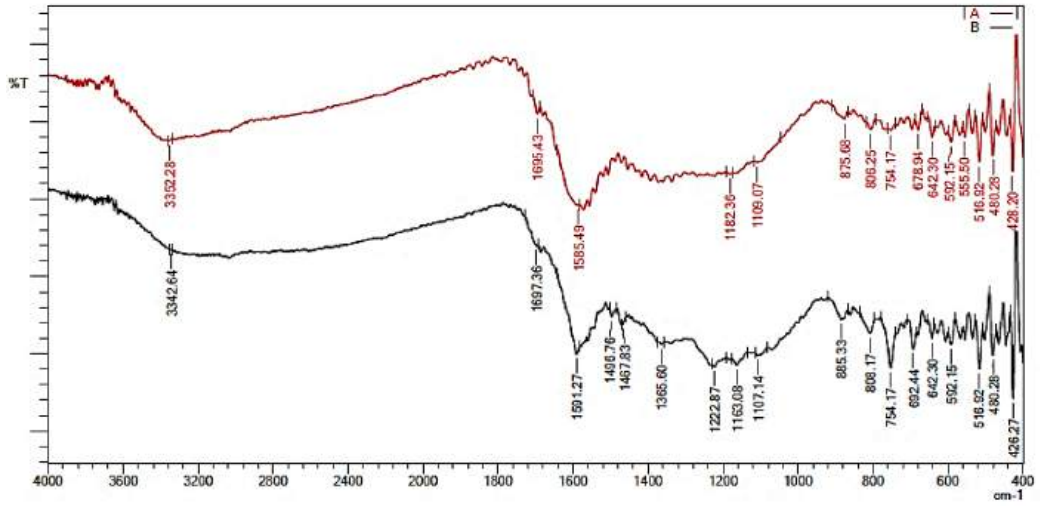

Figure 5. FTIR analysis of nano-activated carbon biosynthesized (A) before (B) and after adsorption.

related to the stretching vibrations of C−H [Veerapandian et al., 2015]. Finally, some differences in absorbance peaks were noticed after nanoscale AC adsorption of phenol from synthetic wastewater, because of the relationship between phenol and functional groups of the adsorbent.

Experimental design

The four distinct factors of (A) phenolic contaminant content, (B) pH, (C) dose adsorbent concentration, and (D) time were studied utilizing statistical analysis and experiment design, data analysis (Design Expert Software), Statistical, Ease Inc., Minneapolis, MN, USA 7.0) and a central composite design (CCD) using a response surface methodology (RSM) [Ozbay and Yargic, 2015]. The program was used to create graphs and calculate effects that perform variance analysis, where responses and factors are two categories of variables used in the optimization process [Shakor et al., 2022]. The use of the response surface method in many chemical and physical processes to build a series of tests is a clear and simple way to choose the most appropriate practical experiments. In this work, four process variables were linked to the operation, namely initial phenol concentration, pH solution, adsorbent dose, and content time. The ratios of these variables were improved to remove phenol. Four variable components and three levels were used in the study, ranging from (-1) minimum, average (0), to (+1) maximum as indicated in Table 1. Table 2 illustrates the specific data for each of the 30 runs [AbdulRazak et al., 2018].

Regression model equation

To incorporate only significant factors in the models, the experimental findings for phenol removal were modelled by applying the backward regression method. This process was carried out automatically using Design Expert 7.0.0. The following factors, encoded as an equation of second-order polynomial quadratic, were used to build the model for phenol elimination (response). Where A represents the initial concentration (ppm) of phenol, B is the solution pH, C is the adsorbent dose (ppm), and D indicates the contact period (minutes). Positive signals in the suggested model denote an increase in the phenol removal ratio caused by these variables, whereas negative signs suggest a drop in the response, see Equations 2 and 3.

Table 1. High, central and low levels of the independent variables

Factor	Symbol	Levels		
		-1	0	+1
Initial concentration (ppm)	A	30	75	120
PH	B	2	6.5	11
Dose (ppm)	C	50	325	600
Time (min)	D	30	75	120

Table 2. Experimental design data concerning percentage phenol removal

Std	Run	Factor (1) initial conc. (ppm)	Factor (2) PH	Factor (3) dose (ppm)	Factor (4) time (min)	Response1 adsorption capacity(qe) (mg/g)
2	1	30	11	600	120	7.012
29	2	120	11	50	120	103.85
18	3	120	2	50	30	120.67
3	4	75	6.5	325	75	8.576
23	5	30	11	600	30	3.789
27	6	30	11	50	120	15.355
14	7	30	2	600	30	30.37
13	8	75	6.5	325	75	8.576
11	9	30	2	50	30	55.58
1	10	75	6.5	325	75	8.576
16	11	75	6.5	325	75	8.576
30	12	75	6.5	325	75	8.576
19	13	75	6.5	325	75	8.576
25	14	75	6.5	325	75	8.576
6	15	75	6.5	325	75	8.576
5	16	120	6.5	325	75	9.89
28	17	75	11	325	75	29.9
12	18	120	11	600	120	37.5
24	19	75	6.5	325	75	8.576
17	20	75	6.5	325	30	8.9
4	21	120	2	600	30	38.89
15	22	30	11	50	30	11.39
10	23	120	2	600	120	49.408
20	24	120	2	50	120	125.29
7	25	30	2	600	120	34.92
21	26	75	6.5	325	120	10.2
9	27	120	11	600	30	26.335
22	28	120	11	50	30	91.34
8	29	75	6.5	600	120	8.72
26	30	30	2	50	120	36.82

- Coded equation

$$\text{Adsorption capacity (qe)} = + 7.80 + 24.66A - -12.43B - 20.97C + 1.64D + 2.81AB - - 15.37AC + 2.86\,AD + 2.34\,BC + + 1.87\,BD + 1.48\,CD - 19.06\,A^2 + + 38.04\,B^2 + 20.53\,C^2 + 1.75\,D^2 \quad (2)$$

- Actual equation

$$\text{Adsorption capacity (qe)} = + 62.52038 + + 2.16724\ \text{initial conc.} - 29.531080\ \text{pH} - - 0.180813\ \text{dose} - 0.298267\ \text{time} + 0.013861\ \text{initial conc.}\ \text{pH} - 0.001242\ \text{initial conc. dose} + + 0.001415\ \text{initial conc. time} + 0.001893\ \text{pH dose} + 0.009239\ \text{pH time} + 0.000119\ \text{dose time} - 0.009412\ \text{initial conc.}^2 + 1.87855\ \text{pH}^2 + 0.000271\ \text{dose}^2 + 0.000866\ \text{time}^2 \quad (3)$$

The negative value related to the adsorbent dose (C) and (B) pH of the solution has a negative effect as these terms increase the rate of adsorption capacity. On the contrary, the positive value related to the overlay of primary phenol (A) and content time (D) denotes that it had a positive impact on the adsorption capacity of % phenol.

ANOVA analysis

An ANOVA test was conducted to examine the accuracy and relevance of the current model. The findings are listed in Table 3. With a high F value of 216.64, the value p was set a > 0.05. These results support the idea that the best model for demonstrating the process of phenol elimination

Table 3. The ANOVA results for the phenol removal model

Source	Sum of squares	df	Mean square	F Value	p-value Prob > F	
Model	35159.02	14	2511.36	216.64	< 0.0001	significant
A-initial conc.	9891.01	1	9891.01	853.23	< 0.0001	
B-PH	2513.38	1	2513.38	216.81	< 0.0001	
C-dose	7155.59	1	7155.59	617.26	< 0.0001	
D-time	49.34	1	49.34	4.26	0.0569	
AB	126.06	1	126.06	10.87	< 0.0049	
AC	3781.11	1	3781.11	326.17	< 0.0001	
AD	131.30	1	131.30	11.33	0.0042	
BC	87.76	1	87.76	7.57	0.0148	
BD	56.01	1	56.01	4.83	< 0.0441	
CD	35.43	1	35.43	3.06	0.1008	
A^2	490.39	1	490.39	42.30	<0.0001	
B^2	1953.70	1	1953.70	168.53	< 0.0001	
C^2	320.56	1	320.56	27.65	<0.0001	
D^2	5.14	1	5.14	0.4433	0.5156	
Residual	173.89	15	11.59			
Lack of fit	173.89	7	24.84			
Pure error	0.0000	8	0.0000			
Cor total	35332.91	29				
Std. dev.	5.27		R^2	0.9951		
Mean	32.56		Adjusted R^2	0.9905		
C.V. %	16.20		Predicted R^2	0.9492		
			Adeq Precision	49.5994		

is the second-order quadratic model. Model terms with «Prob > F" values lower than 0.0500 are significant.

In this case, the moel terms A, B, C, D, AB, AD, BC, BD, CD, and B^2. regression coefficients R^2, adapted R^2 and forecast R^2, which were 0.9951, 0.9905 and 0.9492 respectively, were used to assess the correctness of the aforementioned models. These findings suggest that a significant amount of the experimental data may be accounted for.

Figure 6 illustrates the actual percentage of phenol removal values against the predicted values, demonstrating a strong agreement between

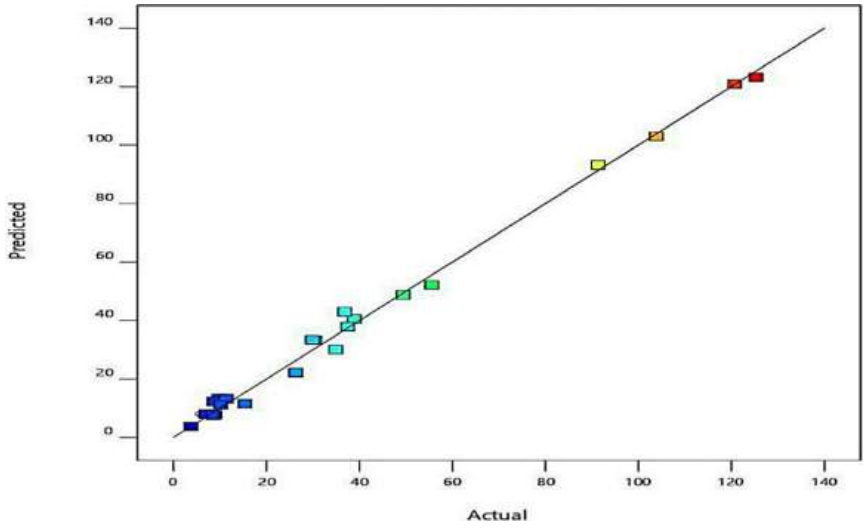

Figure 6. The predicted against the actual percentage of removal phenol

the two sets of data. The influence of the initial concentration of the phenol ion on the performance of the adsorption process was examined. Figure 7 displays the adsorption ratio with various initial concentrations of phenol ions (30–120 ppm), It was clear when the phenol concentrations were increased from 30 to120 ppm, the adsorbent's adsorption effectiveness rose, which is attributed to the adsorbing sites found on the ACNPs surface. The raise in the phenol concentration led to a reduction in the adsorption capacity due to the saturation of active adsorption sites on the surfaces of ACNPs [Younis et al., 2014].

The pH of the solution is a critical factor that affects the absorption of phenol from wastewater. The pH effect on the effectiveness of ACNP-mediated phenol adsorption is presented in Figure 8. The pH values range from 2 to 11, keeping the adsorbent dose of 325 ppm and contact time constant at 75 minutes, with an initial concentration of 75 ppm. Therefore, this section's research aims to determine the ideal pH of modified ACNPs to obtain the best adsorption efficiency when removing phenol from aqueous media. It was observed that the most efficient adsorption of ACNPs for phenol occurred at a pH of 6.5, with pH values over 7 considerably decreasing the adsorption efficacy. An essential part of the adsorption process is played by the active-surface functional groups of nanostructure-activated carbon on ACNPs Mirian and Nezamzadeh-Ejhieh, 2016]. At pH 6.5, it was discovered that the nanomaterial's surface alteration with reed stalks was sufficient to provide a virtually net positive surface charge. Furthermore, positive charges

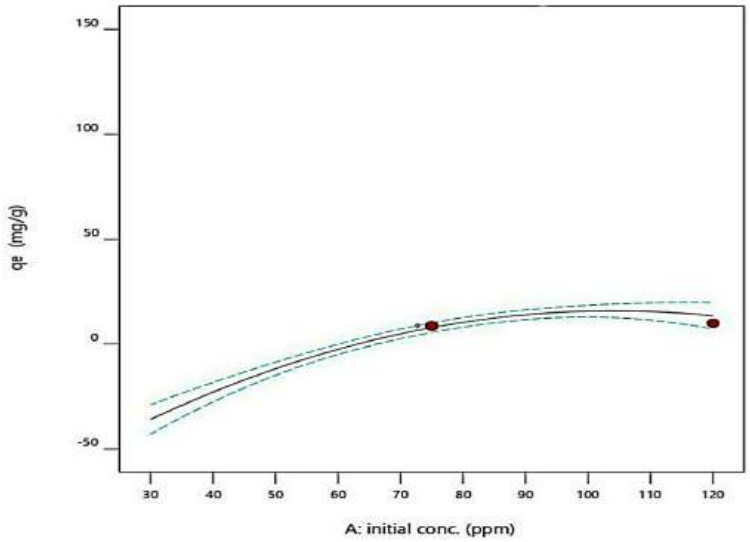

Figure 7. The impact of the initial concentration (ppm) on the adsorption capacity

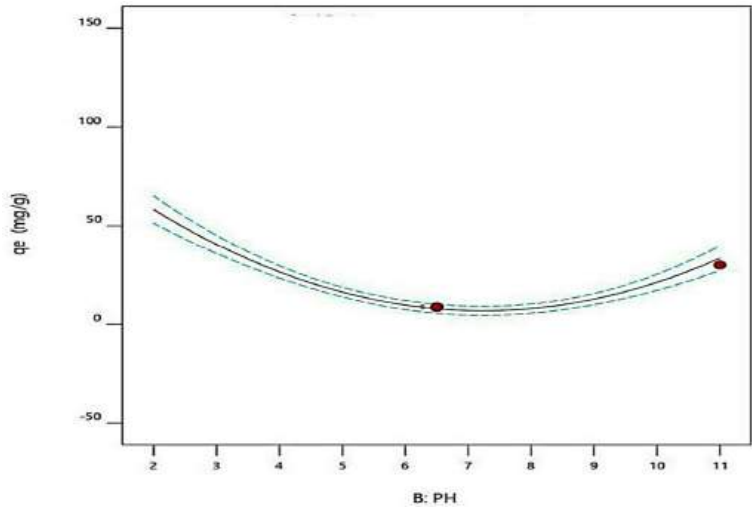

Figure 8. The effect of pH on adsorption capacity

were built up on the surface of the nanomaterial in an acidic condition (pH = 2). Accelerated phenol absorption resulted from these electrostatic exchanges through the negatively emotional surface of the phenol ions. Because of the possible disgusting forces amongst the negative charges on the outward of ACNPs and phenoxide ions, it was seen that the phenol molecules detach in the basic aqueous solution at 11 to create phenoxide ions that were slightly immobilized, disturbing the adsorption process at an acidic environment [Zhang et al., 2018]. Moreover, it was shown that greater repulsive forces between the surfaces of negative ACNPs and phenolic molecules appeared, which led to a reduction in the amount of adsorption, and reduced the removal effectiveness of phenolic pollutants in the basic medium at pH equal to 11 [Aazza et al., 2017]. The effect of nano-activated carbon on the adsorption process is presented in Figure 9. The nano adsorbent concentrations ranged from 50 to 600 ppm. The amount of the removal phenol decreased from 10.2 to 8.72 when the amount of adsorbent was doubled from 325 to 600 ppm). The absorption process sustained to reduction as the adsorbent concentration augmented but at a slower rate. The reduction for phenol adsorbed per unit weight of the adsorbent is probably caused by the concentration difference between the phenol in the bulk and the phenol on the surface of the ACNPs adsorbent. Therefore, as the concentration of the adsorbent increased, the phenol adsorption efficiency decreased [Kumar and Jena, 2016].

The important fundamental elements that affect the effectiveness of adsorption is the effective adsorption time spent in the interaction between the adsorbents. Figure 10 illustrates the removal experiments performed over a range of contact times (30–120 minutes) to investigate the impact of contact duration on the best conditions for adsorbing phenol ions using ACNPs. These experiments were conducted at pH 6.5, with a phenol concentration of 75 ppm, and a 325 ppm nano active carbon adsorbent dose. When the contact time was extended from 30 minutes to two hours, a progressive improvement in the effectiveness of phenol elimination was achieved. The ACNPs showed efficient adsorption of phenol ions compared to previous research on other adsorbents. [Younis et al., 2016]. Bhatnagar, 2007 carried out the bromo phenol adsorption on carbon sorbents made from solid fertilizer waste, and the process reached equilibrium in eight hours. The findings were attributed to the adsorbent having enough unoccupied adsorption sites for the 2 hours of adsorption time, which is the period obligatory to grasp the equilibrium point of adsorption. At this point, the adsorbed saturated surfaces' active sites, and the phenol ions in the aqueous medium did not disappear [Zainudin et al., 2010].

The combined effect of variables on phenol removal

The study examined the removal of phenolic pollutants concerning the initial concentration of phenol, adsorbent dose, reaction time, the ACNPs solution pH, and combined influence of these variables. Plotting the phenol removal percentage versus two independent variables while holding other factors constant resulted in 3D

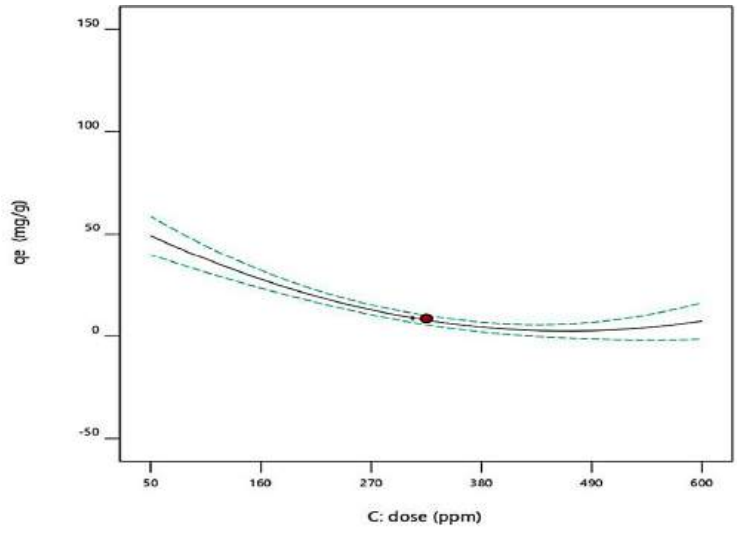

Figure 9. Effect of adsorbent dose (ppm) on the adsorption capacity

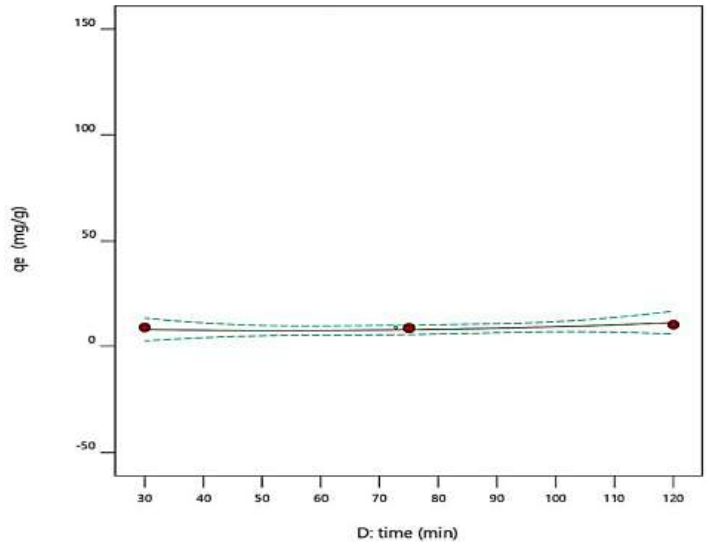

Figure 10. The impact of content time (minutes) on the capacity of the adsorption process

response surface plots. Response surface (3D) plots resembling two-dimensional contour plots can be used to show how independent variables affect response. Figure 11 provides an additional illustration of the pH effect. Sodium hydroxide and diluted hydrochloric acid were employed to alter the solution pH when the pH was over 7, the removal's efficacy dropped, and it was most effective at pH 6.5. The reducing role of Nano carbon in the oxidation-reduction cycle is the cause of the acidic state [Rasheed et al., 2011]. The pollutant can be absorbed onto the surface of the adsorbent molecules more readily at pH 6.5. Reduced phenol removal results from the insoluble forms of ACNPs that diffuse into reactive sites under alkaline conditions. Phenoxide molecules interact with the adsorbent when they are negatively charged in an alkaline environment. The phenoxide ion and (O–H) group are subjected to repulsive forces as a result of this occurrence. Furthermore, the electrostatic repulsive force grows stronger with increasing pH, which slows down adsorption and diffusion. Additionally, the electrostatic repulsive force becomes effective at high pH values because the surface of ACNPs becomes negative. Acidic environments, on the other hand, encourage cleaning metal surfaces. These activities both increase the solubility of these hydroxides and lessen the passivation of carbon nanoparticles [Saharan et al., 2014].

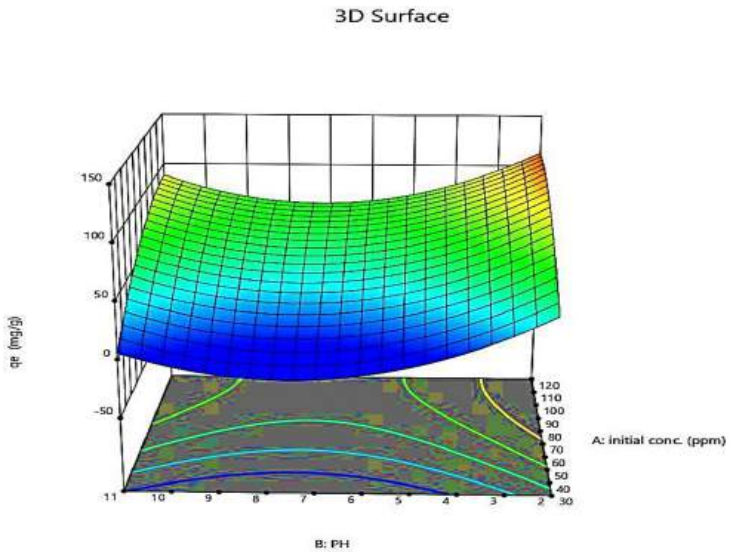

Figure 11. Effect of interaction between initial concentration of phenol and pH on the % adsorption capacity at a constant contact time of 75 min and the adsorbent dose of 72 mg/l

This leads to an enhancement in the breakdown of phenol molecules with adsorbent molecules at low pH. Activated nanocarbon (ACNPs) molecules also have a positive charge at pH 6.5. Ionized phenolic species with negative charges are absorbed by these positive charges.

The impact of the ACNPs adsorbent dosage on the phenol removal was examined by changing the adsorbent dose from 50 to 600 ppm as represented in Figure 12. The phenol removal rate decreased significantly when the adsorbent loading reached 600. The efficiency of removing phenolic pollutants decreased from 120.67 to 38.89 ppm with the other three variables constant. This indicates that increasing the dose of the adsorbent resulted in a decrease in the phenol efficiency, which can occur due to a decrease in the active surface of the adsorbent [Ahmadi and Mostafapour, 2017]. The increase in the adsorbent amount led to higher phenol absorption because of the increased active surface area and active sites of the adsorbent [Sui et al., 2011].

When the contact time was extended, while maintaining the other factors constant, the results indicated that the optimal contact times for phenol removal by active carbon nanoparticles were 120.67 min and 125.59 minutes. The efficiency of phenol elimination was observed to rise with time, reaching a plateau after 120 minutes, as illustrated in Figure 13. The site intercalation between the phenol ion and the surface-active groups is responsible for the phenol elimination within the specified period. Moreover, the enhanced availability at adjacent active locations on the sorbent's surface area explains the extra absorption at the aforementioned times [Ulucan et al., 2013].

The adsorption of primary phenol was also examined in the concentration range from 30 to 120 ppm as clarified in Figure 13. It was noted that increasing the concentration of primary phenol led to an increase in the absorption efficiency, where the absorption efficiency rose from 7.012 to 37.5 with the rise in the initial phenol concentration while keeping the others constant. The removal of phenol by ACNPs depends on the relationship between the phenol and the reactive sites on the surface of the adsorbent [Asmaly et al., 2015].

Figure 14 illustrates the relationship inter alia the adsorbent amount and the pH of the solution remaining the time constant at 75.9 minutes, with 75.9 ppm as an initial phenol concentration. The amount of adsorbent had a detrimental impact on the efficiency of pollutant removal. However, the removal of pollutant efficiency increased as the adsorbent dosage increased across the entire range (2–11) of the solution pH. The adsorbent concentration is considered an essential factor in determining its capacity to adsorb a certain initial phenol. Adsorption tests were conducted using 50 to 120 ppm of adsorbent for 120 minutes, with an initial phenol content of 87.6 ppm, to estimate the impact of adsorbent amount on the adsorption process. It was revealed that when the adsorbent concentration increased as the pH dropped from (2–11), the effectiveness of pollutant removal fell. Moreover, as the adsorbent dose increased, the amount of phenol adsorbent per-

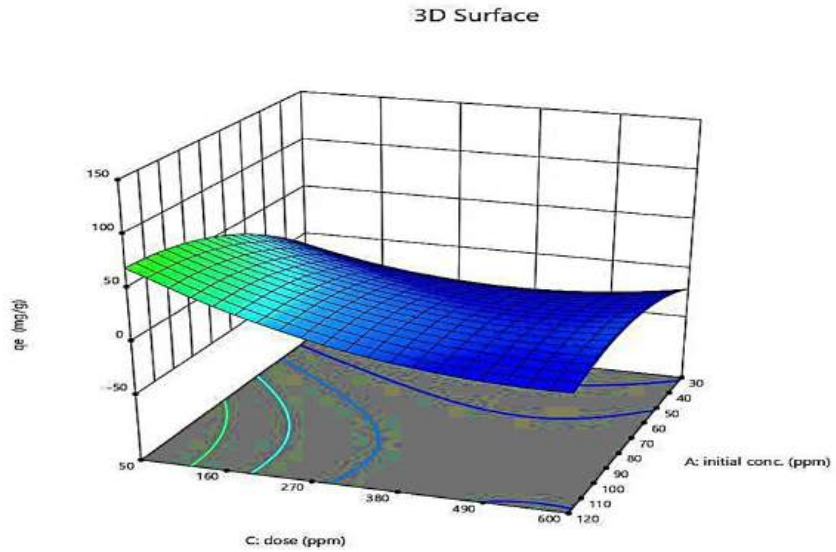

Figure 12. The interaction impact between the initial concentration of the phenol and adsorbent dosage (mg/l) on the % of the capacity of the adsorption process at a contact time of 75.9 min and PH 6.5

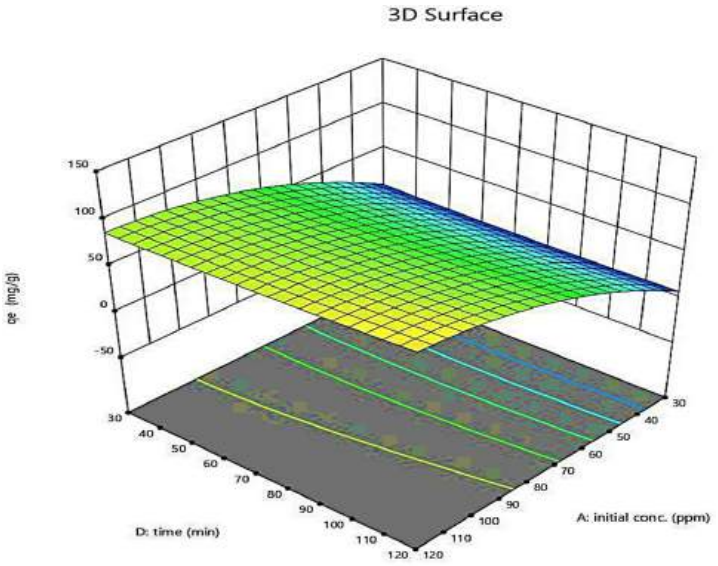

Figure 13. The interaction impact between initial phenol concentration and content time (min) on the % adsorption capacity at an adsorbent dose of 72 ppm and pH 11

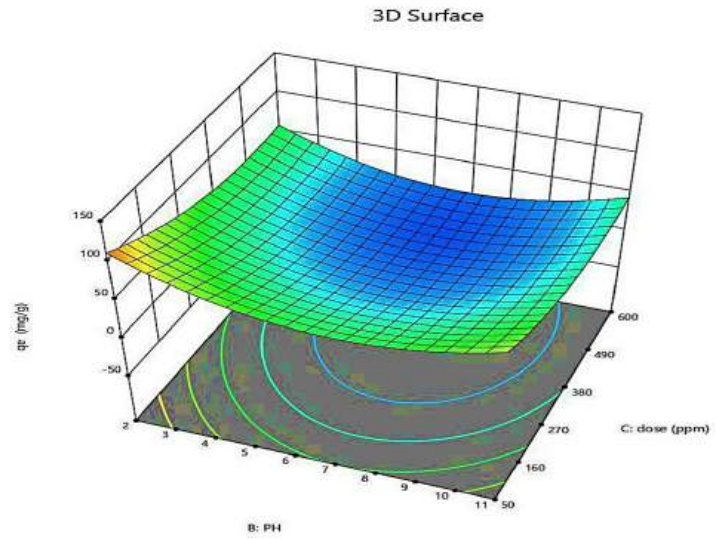

Figure 14. The interaction impact between adsorbent dose and PH on the % adsorption capacity at initial concentration phenol 87.6 (ppm) and content time 120 min

gram of adsorbent (qe) decreased. This is because increasing adsorbent concentrations led to the accumulation of particles and the constant phenol concentration created unsaturated active sites on the adsorbent surface [Chakravarty et al., 2010].

Figure 15 illustrates the impact of simultaneous alterations in pH and contact time, and displays the connection between contact time and pH with constant variables (initial concentration 120 ppm and adsorbent dose 50 ppm). The findings showed that high phenol removal efficiency was achieved by increasing the deposition duration as the pH value decreased. As the pH level drops into the ideal range from 2 to 11 required for the adsorption process, positive charges typically predominate on the surface of active molecules [Hoa and Hue, 2018], leading to the production of colloids and the removal of pollutants [Camacho et al., 2017]. These findings are consistent with those of the results obtained by Boulaadjoul et al., 2018. After 30 min of settling time, researchers found that 97% of the turbidity in the paper mill effluent was eliminated at pH ranges of 2–11. According to Al-Gheethi et al., 2017, phenol treatment effectiveness under lower PH values can be improved by allowing for a settling time of more than one hour.

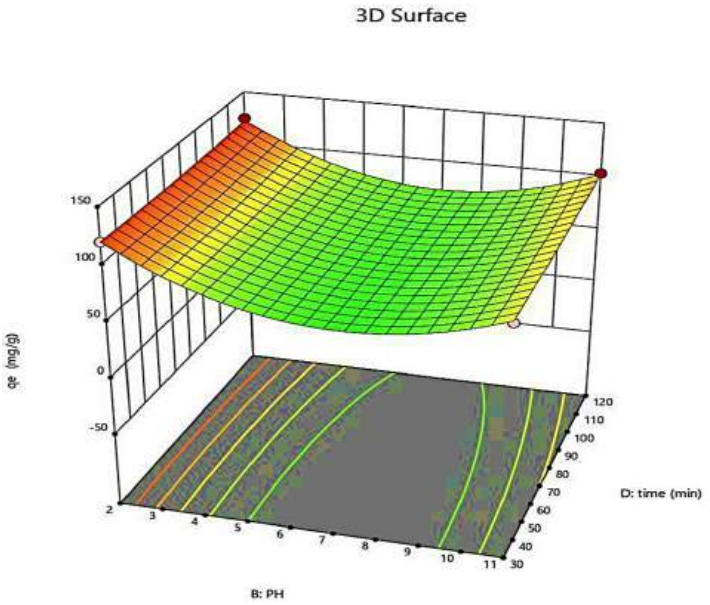

Figure 15. The interaction impact between content time (min) and pH on the % adsorption capacity at initial concentration phenol 120 ppm and adsorbent dose ppm

Optimization of experimental condition

A desirability function was applied to each response and each of the individual elements in the numerical optimization. It was determined the maximum responses with different parameters, initial phenol concentrations of 30 to 120 ppm, contact time of 30 to 120 minutes, and adsorbent doses of 50 to 600 ppm, as well as with a range of pH from 2 to 11. These factors were used to compute the desired values for numerical optimization. Because of the response surfaces' curvature and how they integrate with the want function, a maximum of two targets can be attained when desire is produced randomly [Design Expert Software]. Approximately one hundred optimized conditions were gained within the designed space to achieve high efficiency. Figure 16 shows that the most appropriate option chosen with the best adsorption capacity of the phenol was 30.0825 mg/g at 30 mg/l initial phenol concentration, 600 mg/l adsorbent dose, and 120 min content time at pH = 2 [Tetteh and Rathilal, 2021].

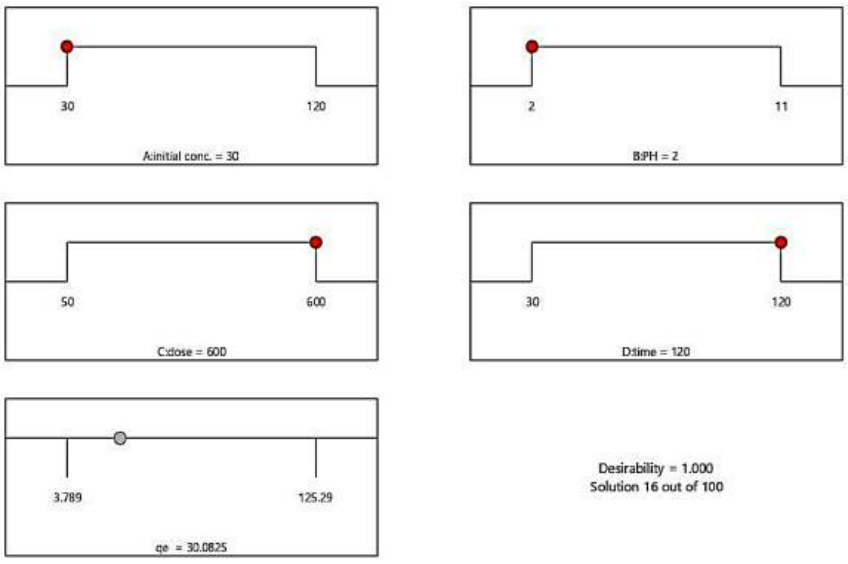

Figure 16. Desirability ramp for the four selected goals numerical optimization

CONCLUSIONS

The study magnificently attained its goal of representing that ACNPs synthesized from reed stalks, a local bio-based material, is an effective adsorbent for removing phenol from contaminated wastewater. Using experimental statistical design, response surface methodology (RSM), and central composite design (CCD), the study identified the optimal conditions for phenol removal, achieving an adsorption capacity of 30.0825 mg/g at a phenol concentration of 30 mg/l, pH of 2, adsorbent dose of 600 mg/l, and contact time of 120 minutes.

The study's outcomes filled a gap in understanding bio-based ACNPs for phenol removal, predominantly with detailed optimization using statistical methods. The use of a second-order quadratic model accurately predicted the phenol elimination process, as evidenced by high regression coefficient values (R^2 = 0.9951, adjusted R^2 = 0.9905, and forecast R^2 = 0.9492). These results validate the model and highlight the potential of this style for emerging efficient, sustainable solutions for wastewater treatment. This study opens up new prospects for using locally sourced, bio-based materials in environmental remediation and provides a framework for further optimization and application of nanomaterials in water purification.

Acknowledgement

The authors would like to express their gratitude to the staff of the Oil and Gas and the Chemical Engineering Departments, University of Technology-Iraq for supporting this work.

REFERENCES

1. Aazza, M., Ahlafi, H., Moussout, H. and Maghat, H., 2017. Ortho-nitro-phenol adsorption onto alumina and surfactant modified alumina: kinetic, isotherm and mechanism. Journal of environmental chemical engineering, 5(4), 3418–3428.
2. Abdul Razak, A.A., Shakor, Z.M. and Rohani, S., 2018. Optimizing Biebrich Scarlet removal from water by magnetic zeolite 13X using response surface method. Journal of environmental chemical engineering, 6(5), 6175–6183.
3. Ahmadi, S. and Kord Mostafapour, F., 2017. Adsorptive removal of aniline from aqueous solutions by Pistacia atlantica (Baneh) shells: isotherm and kinetic studies. J Sci Technol Environ Inform, 5(1), 327–335.
4. Ajala, O.J., Khadir, A., Ighalo, J.O. and Umenweke, G.C., 2022. Cellulose-based nano-biosorbents in water purification. In Nano-Biosorbents for Decontamination of Water, Air, and Soil Pollution, 395–415. Elsevier.
5. Alara, O.R., Abdurahman, N.H. and Ukaegbu, C.I., 2021. Extraction of phenolic compounds: A review. Current research in food science, 4, 200–214.
6. Al-Gheethi, A.A., Mohamed, R.M.S.R., Wurochekke, A.A., Nurulainee, N.R., Rahayu, J.M. and Hashim, M.A., 2017. Efficiency of *Moringa oleifera* seeds for treatment of laundry wastewater. In MATEC web of conferences, 103, 06001. EDP Sciences.
7. Allahkarami, E., Dehghan Monfared, A., Silva, L.F.O. and Dotto, G.L., 2023. Application of Pb–Fe spinel-activated carbon for phenol removal from aqueous solutions: fixed-bed adsorption studies. Environmental Science and Pollution Research, 30(9), 23870–23886.
8. Al-mahbashi, N., Kutty, S.R.M., Jagaba, A.H., Al-Nini, A., Ali, M., Saeed, A.A.H., Ghaleb, A.A.S. and Rathnayake, U., 2022. Column study for adsorption of copper and cadmium using activated carbon derived from sewage sludge. Advances in Civil Engineering, 1, 3590462.
9. Almahbashi, N.M.Y., Kutty, S.R.M., Ayoub, M., Noor, A., Salihi, I.U., Al-Nini, A., Jagaba, A.H., Aldhawi, B.N.S. and Ghaleb, A.A.S., 2021. Optimization of preparation conditions of sewage sludge based activated carbon. Ain Shams Engineering Journal, 12(2), 1175–1182.
10. Al-mahbashi, N.M.Y., Kutty, S.R.M., Jagaba, A.H., Al-nini, A., Sholagberu, A.T., Aldhawi, B.N. and Rathnayake, U., 2023. Sustainable sewage sludge biosorbent activated carbon for remediation of heavy metals: Optimization by response surface methodology. Case Studies in Chemical and Environmental Engineering, 8, 100437.
11. Al-Nini A., Ya H.H., Al-Mahbashi N., Hussin H. 2023. A review on green cooling: Exploring the benefits of sustainable energy-powered district cooling with thermal energy storage. Sustainability. 15(6), 5433. https://doi.org/10.3390/su1506543
12. Asmaly, H.A., Abussaud, B., Saleh, T.A., Gupta, V.K. and Atieh, M.A., 2015. Ferric oxide nanoparticles decorated carbon nanotubes and carbon nanofibers: from synthesis to enhanced removal of phenol. Journal of Saudi Chemical Society, 19(5), 511–520.
13. Azeez, R.A. and Al-Zuhairi, F.K.I., 2022. Biosorption of dye by immobilized yeast cells on the surface of magnetic nanoparticles. Alexandria Engineering Journal, 61(7), 5213–5222.
14. Baikousi, M., Dimos, K., Bourlinos, A.B., Zbořil, R., Papadas, I., Deligiannakis, Y. and Karakassides, M.A., 2012. Surface decoration of carbon nanosheets with

amino-functionalized organosilica nanoparticles. Applied surface science, 258(8), 3703–3709.

15. Bhatnagar, A., 2007. Removal of bromophenols from water using industrial wastes as low cost adsorbents. Journal of Hazardous Materials, 139(1), 93–102.
16. Boulaadjoul, S., Zemmouri, H., Bendjama, Z. and Drouiche, N., 2018. A novel use of *Moringa oleifera* seed powder in enhancing the primary treatment of paper mill effluent. Chemosphere, 206, 142–149.
17. Chai, W.S., Cheun, J.Y., Kumar, P.S., Mubashir, M., Majeed, Z., Banat, F., Ho, S.A., Show, P.L. 2021. A review on conventional and novel materials towards heavy metal adsorption in wastewater treatment application. Journal of Cleaner Production, 296, 126589.
18. Camacho, F.P., Sousa, V.S., Bergamasco, R. and Teixeira, M.R., 2017. The use of *Moringa oleifera* as a natural coagulant in surface water treatment. Chemical Engineering Journal, 313, 226–237.
19. Chakravarty, P., Sarma, N.S. and Sarma, H.P., 2010. Removal of lead (II) from aqueous solution using heartwood of Areca catechu powder. Desalination, 256(1–3), 16–21.
20. Da Silva, M.C., Lütke, S.F., Nascimento, V.X., Lima, É.C., Silva, L.F., Oliveira, M.L. and Dotto, G.L., 2023. Activated carbon prepared from Brazil nut shells towards phenol removal from aqueous solutions. Environmental Science and Pollution Research, 30(34), 82795–82806.
21. de Farias, M.B., Prediger, P. and Vieira, M.G.A., 2022. Conventional and green-synthesized nanomaterials applied for the adsorption and/or degradation of phenol: A recent overview. Journal of Cleaner Production, 367, 132980.
22. Dehmani, Y., Dridi, D., Lamhasni, T., Abouarnadasse, S., Chtourou, R. and Lima, E.C., 2022. Review of phenol adsorption on transition metal oxides and other adsorbents. J Water Process Eng 49, 102965.
23. Ewis, D. and Hameed, B.H., 2021. A review on microwave-assisted synthesis of adsorbents and its application in the removal of water pollutants. Journal of Water Process Engineering, 41, 102006.
24. Fadhil, A.B., Ahmed, A.I. and Salih, H.A., 2017. Production of liquid fuels and activated carbons from fish waste. Fuel, 187, 435–445.
25. Gayathiri, M., Pulingam, T., Lee, K.T. and Sudesh, K., 2022. Activated carbon from biomass waste precursors: Factors affecting production and adsorption mechanism. Chemosphere, 294, 133764.
26. González-García, P., 2018. Activated carbon from lignocellulosics precursors: A review of the synthesis methods, characterization techniques and applications. Renewable and Sustainable Energy Reviews, 82, 1393–1414.
27. Hoa, N.T. and Hue, C.T., 2018. Enhanced water treatment by Moringa oleifera seeds extract as the bio-coagulant: role of the extraction method. Journal of Water Supply: Research and Technology—AQUA, 67(7), 634–647.
28. Johnson, P.J., Setsuda, D.J., Williams, R.S., 1999. Activated carbon for automotive applications. Carbon Mater. Adv. Technol. 235–267.
29. Jun, L.Y., Yon, L.S., Mubarak, N.M., Bing, C.H., Pan, S., Danquah, M.K., Abdullah, E.C. and Khalid, M., 2019. An overview of immobilized enzyme technologies for dye and phenolic removal from wastewater. Journal of Environmental Chemical Engineering, 7(2), 102961.
30. Kumar, A. and Jena, H.M., 2016. Removal of methylene blue and phenol onto prepared activated carbon from Fox nutshell by chemical activation in batch and fixed-bed column. Journal of Cleaner Production, 137, 1246–1259.
31. Kutty, S.R.M., Almahbashi, N.M.Y., Nazrin, A.A.M., Malek, M.A., Noor, A., Baloo, L. and Ghaleb, A.A.S., 2019. Adsorption kinetics of colour removal from palm oil mill effluent using wastewater sludge carbon in column studies. Heliyon, 5(10).
32. Patil, A., Arya, M. Water Quality Assessment and Heavy Metal Analysis of Ganga River System and Effluent Water of SIDCUL at Haridwar through Atomic Absorption Spectroscopy.
33. Leal Filho, W., Shiel, C., Paço, A., Mifsud, M., Ávila, L.V., Brandli, L.L., Molthan-Hill, P., Pace, P., Azeiteiro, U.M., Vargas, V.R. and Caeiro, S., 2019. Sustainable Development Goals and sustainability teaching at universities: Falling behind or getting ahead of the pack?. Journal of Cleaner Production, 232, 285–294.
34. Lee, K.Y., Qian, H., Tay, F.H., Blaker, J.J., Kazarian, S.G. and Bismarck, A., 2013. Bacterial cellulose as source for activated nanosized carbon for electric double layer capacitors. Journal of Materials Science, 48, 367–376.
35. Liang, Q., Liu, Y., Chen, M., Ma, L., Yang, B., Li, L. and Liu, Q., 2020. Optimized preparation of activated carbon from coconut shell and municipal sludge. Materials Chemistry and Physics, 241, 122327.
36. Liu, Y., Liu, X., Dong, W., Zhang, L., Kong, Q. and Wang, W., 2017. Efficient adsorption of sulfamethazine onto modified activated carbon: a plausible adsorption mechanism. Scientific reports, 7(1), 12437.
37. Melo, J.M., Lütke, S.F., Igansi, A.V., Franco, D.S.P., Vicenti, J.R.M., Dotto, G.L., Pinto, L.A.A., Cadaval Jr, T.R.S. and Felipe, C.A.S., 2024. Mass transfer and equilibrium modelings of phenol adsorption on activated carbon from olive stone. Colloids and Surfaces A: Physicochemical and Engineering Aspects, 680, 132628.
38. Mishra, R.K., Mentha, S.S., Misra, Y., Dwivedi, N.

2023. Emerging pollutants of severe environmental concern in water and wastewater: A comprehensive review on current developments and future research. Water-Energy Nexus.

39. Mohammadi, S.Z., Lashkari, B., Khosravan, A. and Fouladi, S., 2022. Synthesis of a new magnetic adsorbent using green tea leaf extract and its application in phenol removal by RSM method. Journal of Materials Science: Materials in Electronics, 33(14), 11212–11226.
40. Moralı, U., Demiral, H. and Şensöz, S., 2018. Optimization of activated carbon production from sunflower seed extracted meal: Taguchi design of experiment approach and analysis of variance. Journal of Cleaner Production, 189, 602–611.
41. Naji, S.Z. and Tye, C.T., 2022. A review of the synthesis of activated carbon for biodiesel production: Precursor, preparation, and modification. Energy Conversion and Management: X, 13, 100152.
42. Oruç, Z., Ergüt, M., Uzunoğlu, D. and Özer, A., 2019. Green synthesis of biomass-derived activated carbon/Fe-Zn bimetallic nanoparticles from lemon (*Citrus limon* (L.) Burm. f.) wastes for heterogeneous Fenton-like decolorization of Reactive Red 2. Journal of Environmental Chemical Engineering, 7(4), 103231.
43. Ozbay, N. and Yargic, A.S., 2015. Factorial experimental design for Remazol Yellow dye sorption using apple pulp/apple pulp carbon–titanium dioxide cosorbent. Journal of Cleaner Production, 100, 333–343.
44. Qiu, B., Shao, Q., Shi, J., Yang, C. and Chu, H., 2022. Application of biochar for the adsorption of organic pollutants from wastewater: Modification strategies, mechanisms and challenges. Separation and Purification Technology, 300, 121925.
45. Qasem, N.A., Mohammed, R.H., Lawal, D.U. 2021. Removal of heavy metal ions from wastewater: A comprehensive and critical review. Npj Clean Water, 4(1), 1–15.
46. Roberts, S.M., James, R.C., Williams, P.L. (Eds.). 2022. Principles of toxicology: environmental and industrial applications. John Wiley & Sons.
47. Ragothaman, A. and Anderson, W.A., 2017. Air quality impacts of petroleum refining and petrochemical industries. Environments, 4(3), 66.
48. Rasheed, Q.J., Pandian, K. and Muthukumar, K., 2011. Treatment of petroleum refinery wastewater by ultrasound-dispersed nanoscale zero-valent iron particles. Ultrasonics Sonochemistry, 18(5), 1138–1142.
49. Riyanto, C.A., Ampri, M.S. and Martono, Y., 2020. Synthesis and characterization of nano activated carbon from Annatto Peels (*Bixa orellana* L.) viewed from temperature activation and impregnation ratio of H_3PO_4. EKSAKTA: Journal of Sciences and Data Analysis, 44–50.
50. Saeed, A.A.H., Harun, N.Y., Sufian, S., Siyal, A.A., Zulfiqar, M., Bilad, M.R., Vagananthan, A., Al-Fakih, A., Ghaleb, A.A.S. and Almahbashi, N., 2020. Eucheuma cottonii seaweed-based biochar for adsorption of methylene blue dye. Sustainability, 12(24), 10318.
51. Saharan, P., Chaudhary, G.R., Mehta, S.K. and Umar, A., 2014. Removal of water contaminants by iron oxide nanomaterials. Journal of Nanoscience and Nanotechnology, 14(1), 627–643.
52. Saleh, S., Younis, A., Ali, R. and Elkady, E., 2019. Phenol removal from aqueous solution using amino modified silica nanoparticles. Korean Journal of Chemical Engineering, 36, 529–539.
53. Shakor, Z.M., AbdulRazak, A.A. and Shuhaib, A.A., 2022. Optimization of process variables for hydrogenation of cinnamaldehyde to cinnamyl alcohol over a Pt/SiO_2 catalyst using response surface methodology. Chemical Engineering Communications, 209(6), 827–843.
54. Singh, R.L. and Singh, R.P. eds., 2019. Advances in biological treatment of industrial waste water and their recycling for a sustainable future 225–66. Singapore: Springer.
55. Saravanan, A., Kumar, P.S., Jeevanantham, S., Karishma, S., Tajsabreen, B., Yaashikaa, P.R., Reshma, B. 2021. Effective water/wastewater treatment methodologies for toxic pollutants removal: Processes and applications towards sustainable development. Chemosphere, 280, 130595.
56. Sui, Q., Huang, J., Liu, Y., Chang, X., Ji, G., Deng, S., Xie, T. and Yu, G., 2011. Rapid removal of bisphenol A on highly ordered mesoporous carbon. Journal of Environmental Sciences, 23(2), 177–182.
57. Tetteh, E.K. and Rathilal, S., 2021. Application of magnetized nanomaterial for textile effluent remediation using response surface methodology. Materials Today: Proceedings, 38, 700–711.
58. Ulucan, K., Noberi, C., Coskun, T., Ustundag, C.B., Debik, E. and Kaya, C., 2013. Disinfection by-products removal by nanoparticles sintered in zeolite. Journal of Clean Energy Technologies, 1(2), 120–123.
59. Veerapandian, M., Lévaray, N., Lee, M.H., Giasson, S. and Zhu, X.X., 2015. Glucosamine-anchored graphene oxide nanosheets: Fabrication, ultraviolet irradiation, and electrochemical properties. ACS Applied Materials & interfaces, 7(27), 14552–14556.
60. Wang, W., Xiong, P., Zhang, H., Zhu, Q., Liao, C., Jiang, G. 2021. Analysis, occurrence, toxicity and environmental health risks of synthetic phenolic antioxidants: A review. Environmental Research, 201, 111531.
61. Younis, A.M., Kolesnikov, A.V. and Desyatov, A.V., 2014. Efficient removal of La (III) and Nd (III) from aqueous solutions using carbon nanoparticles. American Journal of Analytical Chemistry, 5(17), 1273.

62. Younis, A.M., Nafea, E.M., Mosleh, Y.Y. and Hefnawy, M.S., 2016. Low-cost biosorbent (*Lemna gibba* L.) for the removal of phenol from aqueous media. Journal of Mediterranean Ecology, 14, 55–62.
63. Zainudin, N.F., Abdullah, A.Z. and Mohamed, A.R., 2010. Characteristics of supported nano-TiO2/ZSM-5/silica gel (SNTZS): photocatalytic degradation of phenol. Journal of hazardous materials, 174(1–3), 299–306.
64. Zhang, L., Liu, P., Li, L., Huang, Y., Pu, Y., Hou, X. and Song, L., 2018. Identification and antioxidant activity of flavonoids extracted from Xinjiang jujube (*Ziziphus jujube* Mill.) leaves with ultra-high pressure extraction technology. Molecules, 24(1), 122.
65. Zhang, L.J., Qian, L., Ding, L.Y., Wang, L., Wong, M.H., Tao, H.C. 2021. Ecological and toxicological assessments of anthropogenic contaminants based on environmental metabolomics. Environmental Science and Ecotechnology, 5, 100081.